Overtone spectroscopy of formic acid

ARTICLE *in* CHEMICAL PHYSICS · OCTOBER 2002

Impact Factor: 1.65 · DOI: 10.1016/S0301-0104(02)00507-4

ELSEVIER

Chemical Physics 283 (2002) 47–61

Chemical Physics

www.elsevier.com/locate/chemphys

Overtone spectroscopy of formic acid

M. Freytes [a,1], D. Hurtmans [a,2], S. Kassi [a,3], J. Liévin [a], J. Vander Auwera [a,4], A. Campargue [b], M. Herman [a,*]

[a] *Laboratoire de Chimie Physique Moléculaire CP 160/09, Université Libre de Bruxelles, Roosevelt Ave. 50, B-1050, Bruxelles, Belgium*
[b] *Laboratoire de Spectrométrie Physique (associated with CNRS UMR C5588), Université Joseph Fourier de Grenoble, B.P. 87, 38402 Saint-Martin-d'Hères Cedex, France*

Received 20 November 2001

Abstract

Vibrational assignments of fundamental, combination and overtone bands in the main isotopomer of gaseous *trans*-formic acid are reported from spectra either newly or previously [J. Chem. Phys. 113 (2000) 1535] recorded using high-resolution Fourier transform and intracavity laser absorption spectroscopies. A total of 62 bands, with 32 newly reported ones, are observed from the lowest energy band, ν_7 at 626.16 cm^{-1} up to $4\nu_1$ at 13284.1 cm^{-1}. Among these bands, 43 are firmly assigned, and 16 tentatively. Effective vibrational constants are obtained. The normal modes of vibrations are further characterised using ab initio calculations providing fundamental band intensities and picturing normal mode nuclear displacements. The effective investigation of the rotational structure in the first CH stretch overtone band ($2\nu_2$) and in the second OH stretch overtone band ($3\nu_1$) is detailed. Rotational information is also presented for $3\nu_2$ and two close-lying bands, that could be extracted from the strong overlapping formic acid dimer bands using artificial filtering procedures.

1. Introduction

The investigation of vibration–rotation structures in organic compounds in their *ground* electronic state fulfills a number of motivations. In the first place, it stimulates both optimal instrumental and extended theoretical developments to systematically cope with prohibitively large rotational line density. In this respect, such investigations contribute pushing away the intrinsic limitations of high-resolution molecular spectroscopy in terms of resolving and assigning vibration–rotation lines in ever-larger species. In the second place, the results of the study of vibration–rotation structures in organic compounds in their

* Corresponding author.
E-mail address: mherman@ulb.ac.be (M. Herman).

[1] On temporary leave from CEILAP Centro de Investigaciones en Láseres y Aplicaciones (CITEFA, CONICET), Zufriategui 4380, 1603-Villa Martelli Buenos Aires, Argentina.

[2] Senior Research Assistant with the Fonds National de la Recherche Scientifique, Belgium.

[3] EU postdoc. (contract SPHERS HPRN-CT-2000-00022), Belgium.

[4] Research Associate with the Fonds National de la Recherche Scientifique, Belgium.

0301-0104/02/$ - see front matter
PII: S0301-0104(02)00507-4

ground electronic state may provide the necessary information to detect in the infrared and near-infrared spectral ranges larger and the so-called prebiotic compounds in non-terrestrial environments. Given recent instrumental developments, these fields are of increased relevance, in the interstellar context in particular. Next, extended data on the vibrational structure, if supported by reliable rotational information, give access to omnipresent intramolecular couplings, possibly allowing unravelling them and, hopefully, searching for general rules, if any, to deal with the vibrational energy pattern in larger species. These rules involve new vibrational co-ordinates more appropriate than traditional normal modes. Such investigations of the rovibrational energy pattern certainly raise fundamental questions about statistical and non-statistical behaviours. The latter concept, if applicable at chemically significant energies, is the key to selective overtone induced chemistry. Eventually, clustering of organic species may occur even under low-pressure conditions, e.g., through hydrogen bonding, and be studied using high-resolution infrared spectroscopy. This provides another, important motivation in this field.

The infrared literature over the last 10 years demonstrates a number of achievements along these lines, as illustrated or summarised, e.g., in [1–13]. These various results definitely demonstrate that the investigation of vibration–rotation structures in organic compounds in their ground electronic state brings forward a number of features of interest to remote sensing, to intra- and actually also inter-molecular dynamics, and more generally to chemistry.

This paper is devoted to formic acid (HCOOH). Although of rather small size compared to other compounds considered in this special issue of Chemical Physics, this species exhibits many interesting features along the lines just highlighted, as revealed by high-resolution infrared spectroscopy. It is observed in our atmosphere and in various astrophysical objects, see, e.g., respectively, in [14] and [15,16]. Very recent, infrared and microwave spectroscopic contributions considering the lowest energy vibrations [17,18] are motivated by monitoring applications.

In the present paper, we are adopting the same research strategy as in some of our previous papers, devoted to the study of the infrared spectrum of even larger species, as ethylene [19], propyne [20] and pyrrole and furan [21]. We investigate systematically the vibrational structure in the absorption spectrum, recorded using Fourier transform spectroscopy (FTS) over a spectral range as broad as possible towards the overtone region. Ab initio calculations help in this process. Ultra-sensitive intracavity laser absorption spectroscopy (ICLAS) is furthermore performed to bring dedicated information in the higher excited overtone region of the spectrum. For most bands, the rotational structure is considered, as a help to the vibrational assignment. In some cases, the rotational structure is more deeply investigated, though, in formic acid, extensive perturbations severely limit the line-by-line assignment and detailed fitting procedures. Attempts to unravel the line density from FTS-jet cooled techniques, as reviewed in [22], could unfortunately not be attempted within the present study, but are planned in the near future. At the same time, extensive literature coverage is achieved and significant previous results highlighted. In particular, results from one of our previous contributions, concerning the high-resolution analysis of the $n\nu_{OH}$ excitation series in formic acid [9], are recalled in this paper. The latter study indeed emphasised an overtone induced tautomerism process, which ideally illustrates connection between high-resolution spectroscopy and overtone chemistry. Eventually, we also briefly report on the dimer of formic acid in the present paper, observed on the spectrum even under low-pressure and room temperature conditions.

More specifically, in Section 2, fundamental bands are discussed, from the results of ab initio calculations and from experimental observations. Experimental procedures are then presented, in Section 3. Next, in Section 4, the assignment of vibrational bands is discussed and vibrational constants are reported. Detailed information, including rotational analyses, is presented in Sections 5 and 6 concerning the CH and OH overtone series, respectively, before concluding in Section 7.

2. Fundamental vibrations

Formic acid, HCOOH, is a planar molecule whose symmetry fits the C_s point group. It has two rotamers, *cis* and *trans* [23]. The *trans*-form, which has two hydrogen atoms opposite with respect to the C–O bond, is 1000 times more abundant than the *cis*-form at room temperature ([24,25] and Refs. therein). Related geometrical parameters were reported from experimental [26–28] and ab initio investigations [9,29]. Only that *trans*-rotamer seems to be observed in the spectra we have recorded and is thus dealt with in the present work. *Trans*-formic acid is a slightly asymmetric, strongly prolate rotor ($\kappa = -0.95$), whose ground state rotational constants in A-reduced, I^r representation [30] were provided in [9]. Unstructured broad bands arising from the dimer [31–34] are also observed on the present spectra, some of them briefly discussed in Section 6.

Table 1 lists experimental fundamental band origins, selecting values from the literature whenever more precise than those resulting from the present work, presented in Section 4. The calculated normal modes of vibration are depicted in Fig. 1 from ab initio calculations performed at the MP2/aug-cc-pVTZ level of theory using Gaussian98 [35], apparently for the first time in the literature. The arrows in Fig. 1 correspond to mass weighted Cartesian normal co-ordinates normalised to 1 ($\sqrt{\text{amu}}$ Å).

Table 1
Experimental fundamental band origins ($\tilde{\nu}_0$ in cm^{-1}), and ab initio calculated integrated intensities of fundamental bands (A_i in km mole^{-1}) in *trans*-formic acid, in the ground electronic state

Mode	$\tilde{\nu}_0$ (experimental)	A_i (calculated)
ν_1	3570.5[a]	79
ν_2	2942.06[b]	31
ν_3	1776.83340[c]	332
ν_4	1380[f]	1.3
ν_5	1223[f]	16
ν_6	1104.8521[d]	264
ν_7	626.1656[e]	41
ν_8	1033.469[d]	3.7
ν_9	640.7251[e]	134

[a] [9].
[b] [36].
[c] [37].
[d] [38] see also [17,39].
[e] [18].
[f] This work.

The recent ab initio calculations already mentioned [9,29] produced frequencies of the normal modes of vibration, not repeated here. We are instead presenting in Table 1, in addition to experimental frequencies, IR fundamental band intensities calculated in the present work within the harmonic electric dipole approximation, at the MP2/aug-cc-pVTZ level of theory. The integrated intensity, A_i in km mole^{-1}, of the ν_i fundamental band is defined according to the following equation:

$$A_i = \frac{N_A \pi}{3c^2}\left(\frac{\partial \mu}{\partial q_i}\right)^2, \tag{1}$$

with N_A the Avogadro number and c the velocity of light. The accuracy of these intensity values is estimated to some 30%.

3. Experiments

3.1. FT data

In the first place, we used the spectral data reported in the work previously mentioned [9]. They cover the range 1800–8700 cm^{-1}. For completeness, let us recall that these were recorded using a Bruker IFS120HR FTS with appropriate optics. The sample was obtained from Merck (stated purity > 98%) and introduced at 12.3 hPa pressure in a multipass White-type cell set at 240 cm total absorption path. Some 400 scans were recorded at the time at 0.03 cm^{-1} instrumental resolution (defined as 0.9/maximum optical path difference), coadded and apodised using a Norton–Beer-weak function. A transmittance spectrum was obtained from the ratio with a background spectrum recorded using an empty cell, at the same instrumental resolution. The spectrum was not specifically calibrated, leading to an accuracy of the line positions estimated to about 0.02 cm^{-1} [40]. Most band origins reported in the forthcoming sections were measured from this spectrum. A large portion of the spectrum is presented in Fig. 2.

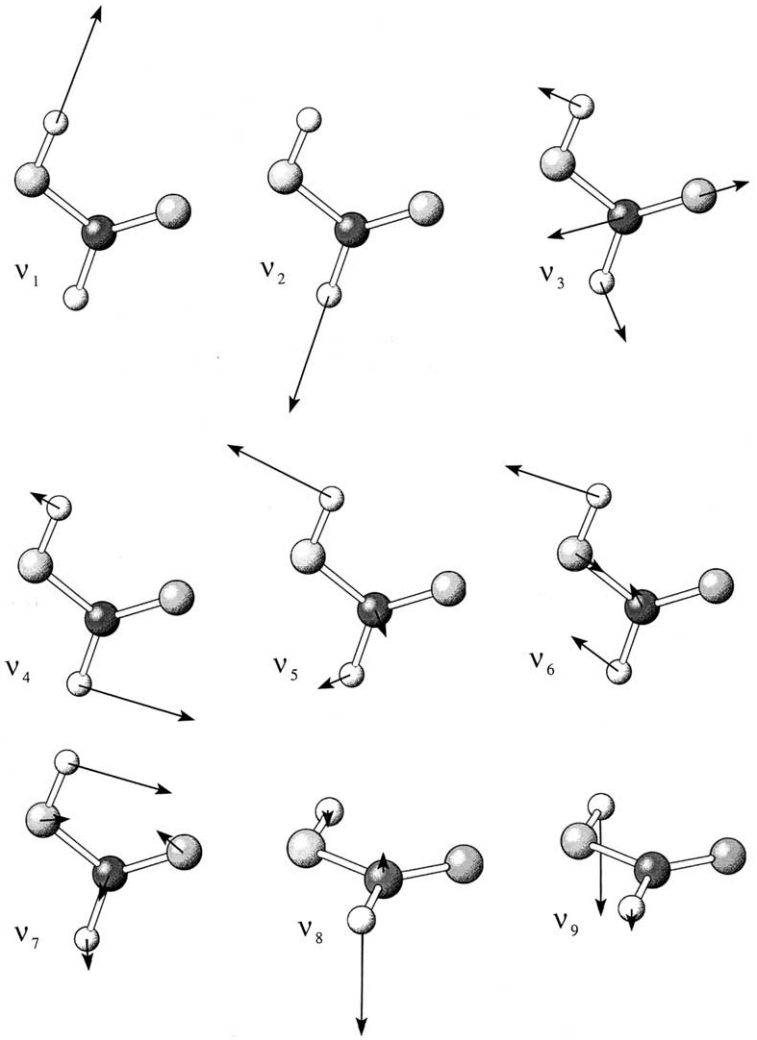

Fig. 1. Normal modes of vibration of *trans*-formic acid, from ab initio predictions at the MP2 level of calculation using aug-cc-pVTZ basis set.

For the present study, we recorded numerous additional absorption spectra to cover the whole range 560–11500 cm^{-1}. The absorption pathlength (L) and cell pressure conditions (P) were adapted to optimally match the various band intensities, and higher resolution was used in some cases. Altogether, in the present work, the pressure was varied between 0.5 and 39 hPa, the absorption pathlength between 21.1 and 4826 cm, the resolution between 0.03 and 0.002 cm^{-1}, and the number of co-added scans between 100 and 700. Sets of conditions applying to specific case studies are highlighted hereafter:

- Rotational parameters on $2\nu_2$, i.e. the first ν_{CH} overtone band, were obtained from the analysis of a spectrum recorded using 240 cm absorption pathlength and 12.3 hPa pressure, at 0.03 cm^{-1} instrumental resolution.
- Rotational parameters on $3\nu_1$, i.e. the second ν_{OH} overtone band, were obtained from the analysis of a spectrum recorded using 4826 cm absorption pathlength and 39 hPa pressure, at

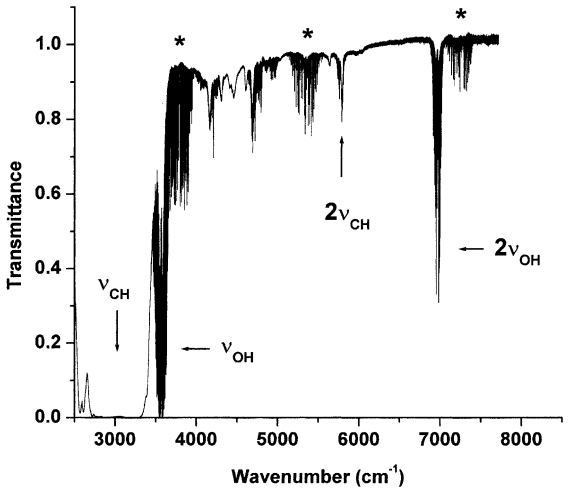

Fig. 2. Overview of the FT transmittance spectrum of *trans*-formic acid between 2500 and 8000 cm^{-1}. Main experimental conditions are 240 cm absorption pathlength and 12.3 hPa pressure. The CH and OH fundamental and first overtone bands are identified on the spectrum. Spectral features marked with a * are due to absorption from H_2O present in the FTS and, probably, in the cell, not properly cancelling out in the transmittance procedure.

0.019 cm^{-1} instrumental resolution. These data were actually merged with ICLAS ones to perform the rotational analysis of this band, detailed in Section 6.2.

- The ranges 570–800 cm^{-1} and 1000–1650 cm^{-1}, the latter being of interest to atmospheric detection, were recorded unapodised and with resolution up to 0.002 cm^{-1}, using dedicated wavenumber calibration; The rotational analysis of the lower of these energy ranges is reported in another contribution [18].
- Dimer formation could be partly controlled by varying the pressure and pathlength conditions, except for weaker monomer bands whose observation required higher pressure conditions (up to 39 hPa) and was therefore always accompanied by stronger dimer absorption.

As a general comment on the FT experiments, pressure was observed to decrease in the cell during the experiments, most likely due to adsorption on the cell walls. In some cases, formic acid was continuously added to maintain reasonably constant pressure conditions. The infrared spectra did not show evidence of formation of any compound even under the highest pressure conditions we have used. Unexpectedly, however, we identified the ν_3 fundamental band of CS_2, most likely present as an impurity in the sample.

3.2. ICLAS data

Concerning ICLAS, we previously recorded the spectrum of the $4\nu_1$ band between 13200 and 13350 cm^{-1} with an equivalent absorption path length of 82.8 km [9]. The spectrum of the $3\nu_1$ band was recorded during the present work using the same Ti: sapphire type laser. Thanks to the higher intensity of this lower overtone band, the equivalent absorption path was limited to about 5 km.

Compared to the FT data, the sensitivity was improved and lower pressure conditions were therefore required, of the order of 1 hPa. As a consequence, the resolution could be increased, up to 0.03 cm^{-1}, and additional details of the rotational structure of the $3\nu_1$ band were observed with ICLAS. The FT measurements were used to calibrate the ICLAS data, to make the procedure easier.

4. Vibrational assignments and constants

4.1. Vibrational assignments

Various studies were already published in the literature about the assignment of the vibration–rotation bands in *trans*-formic acid in the overtone region, e.g., [31,32,41–47], which we used to start the assignment procedure. Table 2 lists all vibrational bands we observed on the present spectra. Besides one band reported by Morita and Nagakura at 4178 cm^{-1} [31], which we could not spot, and two bands overlapping the fundamental ν_1 band very recently observed under very cold jet conditions [48], all other bands previously reported were observed. In addition, 32 new bands were observed. Whenever rotational analysis was either conducted from the present data, as discussed in the following sections, or previously reported, as for $2\nu_1$ and $4\nu_1$ [9] and, also, for some fundamental bands (see Table 1), the band origin resulting from the rotational analysis is

Table 2
Vibrational band assignment in the absorption spectrum of *trans*-formic acid, in the ground electronic state

$\tilde{\nu}_0(cm^{-1})$	Band	Relative intensity/ Q branch
626.16	ν_7	50/
640.72	ν_9	74/
1033.47	ν_8	9/–
1104.85	ν_6	90/s
1223	ν_5	32/–
1255[b]	$(2\nu_7)$	11/–
1306.2[b]	$(2\nu_9)$	14/s
1380	ν_4	10/–
1776.83	ν_3	100/s
1847.8	$(\nu_5+\nu_7)$	9/s
1931.1[b]	$(3\nu_7)$	1.6/s
2132[b]	$\nu_6+\nu_8$	2/m
2196.3	$2\nu_6$	15/s
2298.6[b]	$(\nu_5+\nu_6)$	6/s
2338[b]		5.5/–
2376[b]	$\nu_3+\nu_7$	2/s
2400.2[b]	$2\nu_5$	4/s
2504[a,b]	$(\nu_4+\nu_6)$	2.5/–
2600[a,b]	$\nu_4+\nu_5$	1/–
2745[b]	$2\nu_4$	2/–
2803[b]	$\nu_3+\nu_8$	1/s
2876.6[b]	$\nu_3+\nu_6$	3.5/s
2942.06	ν_2	70/–
3057[b]	$(2\nu_9+\nu_3)$	0.6/–
3106.5[b]	$(\nu_4+\nu_6+\nu_7)$	0.2/s
3152.3[b]	$\nu_3+\nu_4$	0.2/s
3275[b]	$3\nu_6$	0.5/–
3570.5	ν_1	82/–
3826[b]	$(2\nu_4+\nu_6)$	1/–
3963.6[b]	$\nu_2+\nu_8$	0.2/m
4043.4	$\nu_2+\nu_6$	1.2/w
4192[b,c]	$(\nu_1+\nu_7)$	1.8/–
4209	$(\nu_1+\nu_9)$	5.5/s
4242[a,b]		1.2/–
4300[a,b]	$(\nu_2+\nu_4)$	0.7/–
4450[b]		0.3/–
4515.2[b]	$2\nu_4+\nu_3$	0.2/–
4600[b]	$\nu_1+\nu_8$	0.4/–
4670.4	$\nu_1+\nu_6$	1.6/s
4708	$\nu_2+\nu_3$	3.7/–
4779.9	$\nu_1+\nu_5$	3.8/m
4857	$(\nu_1+2\nu_9)$	1.2/–
4941.8	$\nu_1+\nu_4$	1.3/s
5274.4[b]	$3\nu_3$	0.9/m
5343.4	$\nu_1+\nu_3$	1.3/w
5592[b]	$(\nu_2+2\nu_4)$	0.2/–
5774.59	$2\nu_2$	1.6/–
6439.6[b]	$\nu_2+2\nu_3$	0.3/–
6507.4	$\nu_1+\nu_2$	0.7/w
6773[b]	$(2\nu_2+\nu_8)$	1/s
6968.25	$2\nu_1$	15/m
7124.1	$2\nu_2+\nu_4$	1.1/s
7584	$2\nu_1+\nu_7$	1.8/–
7606.6[b]	$2\nu_1+\nu_9$	2/s
8065.2	$2\nu_1+\nu_6$	0.6/s
8167	$2\nu_1+\nu_8$	0.4/–
8336.38[b]	$2\nu_1+\nu_4$	0.4/m
8453.87	$(2\nu_2+2\nu_4)$	0.3/–
8507.56	$3\nu_2$	0.6/–
8741[b]	$2\nu_1+\nu_3$	0.2/–
10202.81	$3\nu_1$	2/m
13284.08	$4\nu_1$	/s

Band origins with 2 decimals arise from rotational analysis, those with 1 decimal usually rely on the measurement of the position of a central Q branch. Tentative assignments, as discussed in the text in some cases, are set between parentheses. Few bands remain unassigned. The relative band intensity is very roughly estimated from the maximum transmittance value in the P- or R-branch absorption or from the central Q branch, and the related information is merged from different spectra into a single set of numbers, relative to the maximum value, $S(\nu_3)=100$. In some cases, such as $4\nu_1$, exclusively recorded using ICLAS, and for all those bands very strongly overlapped by dimer bands, no relative intensity value is provided. Eventually the presence of a strong (s), medium (m) or weak (w) central Q branch is also indicated, in the last column, while the absence of comment indicates the absence of a central Q branch.

[a] Origin very imprecise.

[b] Band newly reported from the present work.

[c] An additional band at 4178 cm^{-1} is mentioned by Morita and Nagakura [31], not observed on the spectra presently recorded.

listed in Table 2 using two decimal numbers. Otherwise, the origin of the band was measured directly on the present spectra, as corresponding either to the onset of the central Q-branch, for a-type bands, or to the middle of the dip between R- and P-branches, for b-type bands. Due to high line density, the resulting precision is sometimes not better than 1 cm^{-1}, as indicated by the absence of decimal number in Table 2. It is nevertheless always improved compared to previous investigations, even in these less favourable cases.

As repeated in Table 2, the relative band intensity is very roughly estimated from the maximum transmittance value, either in the central Q branch, if any, or in the P- or R-branch absorption, wherever maximum. The information from

different spectra is merged into a single set of relative intensity values, in Table 2, which are referenced to the strongest band, i.e. ν_3, with $S(\nu_3)$ set to 100. In the case of $4\nu_1$, exclusively recorded using ICLAS, and for all those bands very strongly overlapped by dimer bands, no intensity information is provided. For the fundamental bands, the trends from these relative experimental intensity measurements very roughly agree with the ab initio values listed in Table 1, most likely pointing out the uncertainty of the experimental measurements. Discrepancies between CH and OH fundamental band relative intensities are tentatively discussed in Section 6. Eventually the presence of a strong (s), medium (m) or weak (w) central Q branch is also indicated, in the last column of Table 2, while the absence of comment indicates the absence of a central Q branch.

Some spectral regions are dense and a detailed rotational analysis, ideally supported by jet-cooled experimental techniques, would be required to help identifying all overlapping vibrational bands. Table 2 is therefore most certainly incomplete. This statement holds, in particular for the spectral region around 3570 cm^{-1}, which, in addition to ν_1, is likely to present the $2\nu_3$, $\nu_2+\nu_7$ and $\nu_2+\nu_9$ bands with significant intensities (see discussion in Section 6 and in [48]). As revealed by the value of the vibrational frequencies and already pointed out in previous investigations on ν_3 [37,49], several bands can also be expected to overlap in the range around 1780 cm^{-1}. In two other ranges, around 2500 and 4200 cm^{-1}, the number of bands can also hardly be reliably estimated, and the band origins listed in Table 2 are most uncertain.

In addition to being incomplete, some of the assignments provided in Table 2, set between parentheses, are tentative. This comment applies, in particular, to most bands involving the very close frequencies ν_7 and ν_9, on the one hand, and ν_6 and ν_8, on the other hand. In other cases, several assignments could be suggested without decisive selection criteria. None of them is then indicated. Fig. 3 details the assignments on a portion of the spectrum, between 4100 and 5000 cm^{-1}.

Altogether, all bands previously reported in the literature were observed on the spectra we present or previously [9] recorded. The present experimental conditions thus allowed 32 additional bands to be identified. Out of a total of 62 observed bands, 43 are firmly assigned, 16 tentatively and 3 left unassigned.

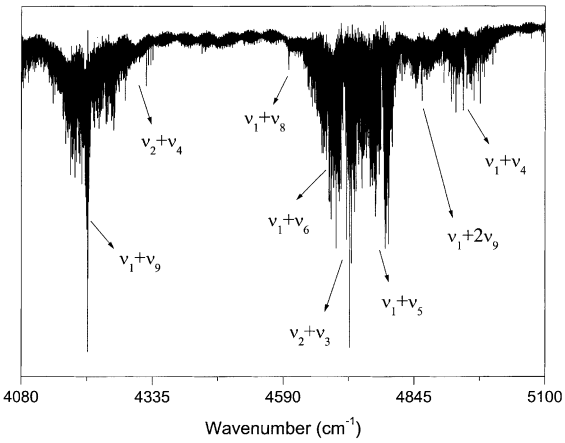

Fig. 3. Portion of the FT transmittance spectrum of *trans*-formic acid in the ground electronic state (4826 cm absorption pathlength, 5 hPa pressure). The $\nu_2+\nu_4$ and $\nu_1+2\nu_9$ assignments are tentative.

4.2. Vibrational constants

We extracted vibrational constants from the band origins listed in Table 2, using, for the overtone bands:

$$G_0(0,0,\ldots,n_i,\ldots,0) = \tilde{\omega}_i^0 n_i + x_{ii}^0 n_i^2 + y_{iii} n_i^3 \qquad (2)$$

or, whenever only the fundamental band was assigned,

$$G_0(0,0,\ldots,1_i,\ldots,0) = \tilde{\nu}_i, \qquad (3)$$

with

$$\tilde{\nu}_i = \tilde{\omega}_i^0 + x_{ii} = \tilde{\omega}_i + 2x_{ii} + 1/2\sum_{j\neq i} x_{ij} \qquad (4)$$

and, for the combination bands,

$$G_0(n\nu_i + m\nu_j + \cdots) = n\tilde{\nu}_i + n(n-1)x_{ii} + m\tilde{\nu}_j + m(m-1)x_{jj} + nmx_{ij} + \cdots \qquad (5)$$

with (all in cm^{-1}): $\tilde{\omega}_i$ the harmonic vibrational frequency, $\tilde{\omega}_i^0$ the harmonic vibrational frequency

referred to the zero point energy level, x_{ii} and x_{ij} the diagonal and non-diagonal anharmonic constants and $\tilde{\nu}_i$ the fundamental vibrational frequency, identical to the fundamental vibrational band origin $\tilde{\nu}_0^i$ in the absence of degeneracy of the vibrational mode, a condition which holds for all modes in planar *trans*-formic acid. In the case of bands starting from the ground vibrational level, G_0 is identical to the band origin, $\tilde{\nu}_0$. In Eq. (2), n_i is the value of the vibrational quantum number v_i and in Eq. (3), n and m are the values of the vibrational quantum numbers v_i and v_j, respectively.

The resulting vibrational constants are provided in Table 3. In all cases, but for the $n\nu_1, n\nu_2$ and $n\nu_6$ series of overtone bands, the constants were determined without any fit, each constant extracted from a single band origin.

All constants are fully effective, meaning that they do not account for perturbations as arising from anharmonic resonances. This effectiveness character applies, in particular for the constants related to the CH (ν_2) excitation since, as explained in Section 5, at least one of the overtone bands ($3\nu_2$) is shifted because of anharmonic coupling in the upper state. This band was nevertheless included in the fitting procedure leading to $\tilde{\omega}_2^0$ and x_{22} (Table 3). As a result, the sum $\tilde{\omega}_2^0 + x_{22}$ (2940.5 cm^{-1}) is different from the fundamental band origin, 2942.06 cm^{-1}. The constants in Table 3 can nevertheless tentatively be used for predictive purposes. They were helpful in the assignment process. For instance, $3\nu_6$ could be precisely predicted with constants determined from lower fundamental and overtone bands in this $n\nu_6$ series, and, among other examples, $2\nu_1 + \nu_4$ was also reliably predicted from $\nu_1 + \nu_4$. None of the tentative assignments was used when determining these vibrational constants.

The rotational structure appears actually well resolved for a number of bands previously not reported at high resolution, or even not reported at all in the literature. However, as experienced at the occasion of the study of the $n\nu_1$ overtone series [9], a detailed high resolution investigation would require improved data, in terms of both resolution and jet-cooled decongestion, and the inclusion of numerous Coriolis-type interactions. As a rule, the exhaustive line-by-line rotational analysis of higher overtone bands of larger polyatomic species, as performed on the lower fundamental bands of *trans*-formic acid [18], becomes unrealistic, given the vibrational level density and the complexity of the coupling network. Nevertheless, vibration–rotation constants were searched for selected bands, from an effective rotational analysis focusing on the less perturbed and congested rotational structures, as reported in the following two sections.

5. Overtone series of CH stretching excitation (ν_2)

5.1. Vibrational analysis

We were able to spot CH stretching ($n\nu_2$) overtone bands up to $n = 3$. As expected, the band intensity decreases with increasing excitation and the experimental conditions had to be adapted. The use of higher pressure and longer pathlength experimental conditions to highlight the shorter wavelength bands also resulted in boosted CH stretching dimer absorption, which could be observed up to $n = 4$. It so happens that the resulting

Table 3
Effective vibrational constants in *trans*-formic acid (cm^{-1}), in the ground electronic state

$\tilde{\omega}_1^0 = 3660.1$	$x_{11}^0 = -91.2$	$x_{12} = -1.8$	$x_{34} = -2.3$
$\tilde{\omega}_2^0 = 2992.9$	$x_{22} = -52.4$	$x_{13} = -1.2$	$x_{36} = -2.6$
$\tilde{\omega}_3^0 = 1786.1$	$x_{33} = -9.3$	$x_{14} = -3.6$	$x_{37} = -13.5$
$\tilde{\omega}_4^0 = 1387.5$	$x_{44} = -7.5$	$x_{15} = -6.1$	$x_{38} = -3.4$
$\tilde{\omega}_5^0 = 1245.9$	$x_{55} = -22.9$	$x_{16} = -1.8$	$x_{45} = -1.5$
$\tilde{\omega}_6^0 = 1111.4$	$x_{66} = -6.6$	$x_{18} = -1$	$x_{68} = -3$
$\tilde{\nu}_7 = 626.2$		$x_{23} = -5.4$	
$\tilde{\nu}_8 = 1033$	$y_{111} = 1.61$	$x_{26} = -1.8$	
$\tilde{\nu}_9 = 640.7$		$x_{28} = -5.7$	

structureless dimer absorption bands are overlapping those of the monomer. This is illustrated in Fig. 4, with all resolved features arising from monomer absorption. The noise level for $n = 4$ forbids identification of monomer absorption. This close similarity in the CH frequencies and anharmonicity in HCOOH and $(HCOOH)_2$ indicates the local character of the CH excitation in both the monomer and the dimer. This could be expected for two main reasons. In the first place, the ab initio picture of the ν_2 normal mode of vibration (see Fig. 1) demonstrates that this excitation corresponds to nuclear displacements fully localised on the CH bond. In the second place, the structure of the symmetric dimer of formic acid, predicted to be most abundant and therefore likely to be responsible of the observed absorption bands, is such that the two CH bonds are symmetrically located on each side of the dimer, pointing outside from the aggregate. The two CH bonds in the dimer are therefore identical and not significantly affected by the dimerisation and furthermore far apart from each other. The related interbond coupling can thus be expected to be negligible and each frequency very similar to that of the monomer, as observed.

As a result of the overlap between monomer and dimer CH bands, the resolved vibration–rotation structures in the monomer are not optimally identified, as demonstrated in Fig. 4. We used the following method to artificially highlight the $n = 3$ absorption band, illustrated in Fig. 5. The fringing in the initial FT spectrum of $3\nu_2$ presented in the lower panel of Fig. 5, was first removed by dividing by an Airy function approximated at first order, giving rise to the spectrum presented in the middle panel of Fig. 5. We then reproduced the baseline shape, including

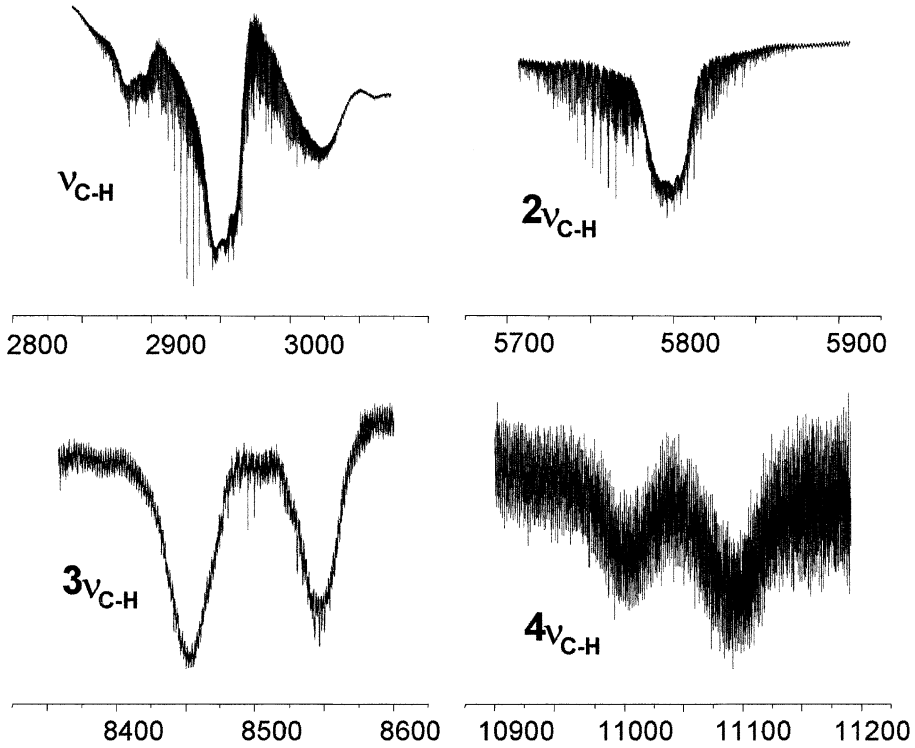

Fig. 4. Spectrum of the $n\nu_2$ overtone bands ($n = 1$–4) of the monomer and dimer of formic acid in the ground electronic state recorded using FTS. The structureless spectral features are from the dimer and the overlapping resolved structures are from the monomer. The absorption pathlength and pressure conditions were as follows: 21.1 cm and 5 hPa ($n = 1$), 4826 cm and 5 hPa ($n = 2$), 4826 cm and 10 hPa ($n = 3$), 4826 cm and 39 hPa ($n = 4$).

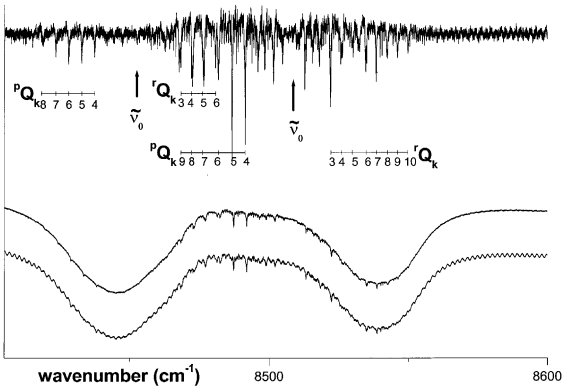

Fig. 5. Illustration of the procedure used to highlight a dark band in *trans*-formic acid borrowing intensity from the $3\nu_2$ bright band ($\tilde{\nu}_0 = 8507.56$ cm^{-1}), tentatively assigned to $2\nu_2 + 2\nu_4$ ($\tilde{\nu}_0 = 8453.87$ cm^{-1}). The lower panel shows the initially recorded FT spectrum. The absorption pathlength and pressure conditions were 4826 cm and 10 hPa, respectively. In the middle panel, the spectrum was divided by an appropriate function to remove instrumental fringing, and further divided, in the upper panel, by the baseline function, thus removing broad and structureless dimer absorption (see text for additional details).

dimer absorption features, using high frequency filtering and phase correction, and further divided the spectrum to remove broad background absorption. We carefully checked that the line positions were unchanged by this procedure. The final result is shown in the upper panel of Fig. 5. The modified spectrum allowed rotational clumps to be identified in $3\nu_2$, as detailed hereafter. It also revealed the presence of an unexpected band borrowing intensity from $3\nu_2$, with the upper resonating state tentatively attributed to $2\nu_2 + 2\nu_4$. This result stimulated a closer investigation of $2\nu_2$ and the same procedure was applied. However, the region is very dense and the origin of the bands and even their number could not be reliably determined.

5.2. Rotational analysis

The $2\nu_2$ band at 5774.59 cm^{-1} is of *b*-type. As shown in Fig. 4, it also presents strong overlap with background absorption from the dimer. The latter was removed using the same procedure as just explained in the previous section, and the rotational structure was analysed. The high line density around the band centre did not allow a detailed analysis to be performed in that range, therefore preventing low-J/K lines to be included in the fitting procedure. A total of 308 vibration–rotation lines were assigned with J/Ka values up to 21/12 and 12/15. The resulting constants are presented in Table 4, from a fit performed using a Watsonian in A-reduced, I^r representation [30], constraining the ground state constants to their value determined in [9]. Although limited to an overview, the comparison between observed and simulated spectra in Fig. 6 highlights both the global reliability and the limitations of the present analysis. A significant number of irregularities were indeed observed in the rotational structure and a large fraction of the lines could not be assigned, or fitted. As already pointed out before, we attribute these problems globally to unidentified interactions with the surrounding bath of zero-order dark states, whose density is roughly just below a few levels/cm^{-1} around 6000 cm^{-1}. Higher quality data, meaning improved instrumental resolution and achievement of spectral simplification, e.g., under supersonic jet conditions, might help further unravelling the fine structure in these bands, although jet-cooled conditions might significantly increase the dimer concentration and, therefore, band overlapping problems. The line wavenumbers and assignments for the $2\nu_2$ band are available from one of the authors (MH).

The $3\nu_2$ band already presented on Fig. 4 is also of *b*-type. Thanks to the procedure previously described and highlighted in Fig. 5, the rotational structure could be partly identified and analysed. We only fitted ^pQ and ^rQ heads, leading to $\tilde{\nu}_0 = 8507.56(4)$ cm^{-1}, and $(A - \bar{B}) = 2.1807(7)$ cm^{-1}. A similar approximate analysis was carried out for the two nearby bands, leading to (in cm^{-1}) $\tilde{\nu}_0 = 8336.38(1)$ and $(A - \bar{B}) = 2.1772(7)$ for $\nu_1 + 2\nu_4$ and $\tilde{\nu}_0 = 8453.87(4)$ and $(A - \bar{B}) = 2.1863(1)$ for the band tentatively assigned to $2\nu_2 + 2\nu_4$. Two of these bands are presented in Fig. 5 which also details their Q branch assignments. All assignments are listed in Table 5. The analysis also revealed additional spectral features around $\nu_1 + 2\nu_4$, which could not be identified.

Table 4
Rotational constants, in cm^{-1}, resulting from the effective rotational analysis of the $2\nu_2$ and $3\nu_1$ bands in *trans*-formic acid

	Ground state*	$2\nu_2$	$3\nu_1$
$\tilde{\nu}_0$	–	5774.591(2)	10202.8084(4)
A	2.58552994	2.56112(9)	2.544282(9)
B	0.402115043	0.40182(8)	0.402978(4)
C	0.347444224	0.34690(9)	0.34772(3)
Δ_J	3.33344×10^{-7}	$-3.9(5) \times 10^{-7}$	$3.7(1) \times 10^{-7}$
Δ_{JK}	-2.87496×10^{-6}	$1.45(4) \times 10^{-8}$	$-1.97(8) \times 10^{-6}$
Δ_K	5.6770×10^{-5}	$2.6(1) \times 10^{-6}$	$5.46(5) \times 10^{-5}$
δ_J	6.4999×10^{-8}	6.4999×10^{-8}*	$-3.8(1) \times 10^{-9}$
		308 lines	458 lines
		rms $= 1.4 \times 10^{-2}$	rms $= 1.9 \times 10^{-2}$

The ground state parameters were constrained to the values of [9]. Additional constants were listed in [9] which, though not printed here, were also used and constrained to the ground state value in both the ground and upper states. The standard deviation (1σ) is indicated in parentheses in the unit of the last quoted digit. The large rms value results from not accounting for numerous observed local perturbations in the model Hamiltonian.

* Constants constrained in the fitting procedure.

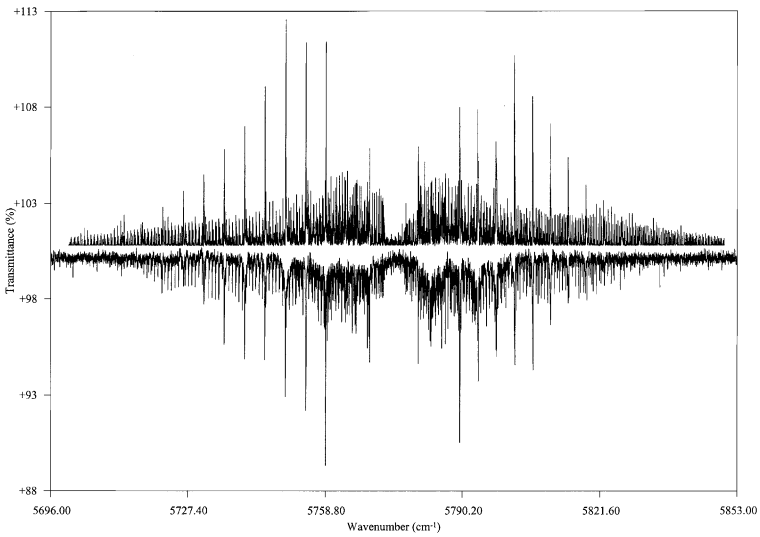

Fig. 6. Overview of the observed (lower trace) and simulated (reversed upper trace) transmittance spectrum of the $2\nu_2$ vibrational band of *trans*-formic acid around ($\tilde{\nu}_0 = 5774.59\ cm^{-1}$). Background absorption from the dimer was artificially removed from the spectrum (240 cm absorption pathlength and 12.3 hPa pressure, at 0.03 cm^{-1} FTS resolution.)

6. Overtone series of OH stretching excitation (ν_1)

6.1. Vibrational analysis

As reported in the previous literature [9,29], most interesting processes are related to the OH stretching overtone excitation. In the first place, possible tautomerism or proton transfer was highlighted from the evolution of the relative *a*/*b* type subband intensity with OH excitation, in [9], involving the progressive shift of the acidic hydrogen nucleus from one oxygen nucleus to the other. Such a mechanism is known to occur at very low energy in longer chain species such as manoladehyde, in which the aldehydic hydrogen is actually equally shared by both terminal oxygen nuclei, thus giving rise to a cyclic compound [50].

Table 5
Assignment of the main Q branches in $3\nu_2$ and accompanying band of *trans*-formic acid, using the notation $^{\Delta K_a}\Delta J_{K''_a}$

K''_a	$3\nu_2$		$2\nu_2 + 2\nu_4$		$2\nu_1 + \nu_4$	
	$^pQ_{K_a}$	$^rQ_{K_a}$	$^pQ_{K_a}$	$^rQ_{K_a}$	$^pQ_{K_a}$	$^rQ_{K_a}$
2					8356.78	
3		8522.55		8468.88		8351.27
4	8492.00	8526.50	8438.20	8473.10	8320.85	8355.47
5	8487.30	8530.50	8433.66	8477.18	8316.05	8359.54
6	8482.41		8428.99	8481.39	8311.36	
7		8538.77	8424.39	8485.22	8306.50	
8	8473.10	8542.67	8419.75		8301.63	
9	8468.28	8546.24			8296.68	
10	8463.36	8550.04			8291.75	

All energies are given in cm^{-1}.

In the second place, dynamical implications of interaction between OH and CH stretching excitation were theoretically investigated using ab initio calculations, considering, in particular, the nearby $5\nu_1$ and $4\nu_1 + \nu_2$ states [29]. Quite similar optimal energy match between members of different overtone series occur at high excitation in a number of species, such as between CH and OH stretching overtones in CH_3OH [51] and in species with CH groups from different chromophores, as in CH_3CHO [52]. In the latter case, the energy match involves members with different excitation values in the overtone series, the n members of the aldehydic CH excitation getting closer to the $n-1$ members of the methyl group overtone, with increasing excitation. Interesting comparison can furthermore be made with similar effects in propyne, which lead in that case to very unusual intensity and homogeneous broadening features [6,20].

As presented in the lower part of Fig. 7, the first overtone band in the $n\nu_1$ (OH) series of bands is stronger than the first overtone band in the $n\nu_2$ (CH) series. This indicates, in first approximation, a larger contribution of the OH vs. CH excitation to the induced electric dipole moment. This trend, confirmed by the next members in the two series in *trans*-formic acid, is currently observed in other species presenting both CH and OH stretching vibrations. As presented in the upper part of Fig. 7, however, the fundamental bands in the two series seem to have very similar strength. According to the ab initio predictions of Table 1, these bands should present an intensity ratio of about 2:1 in favour of ν_1. A closer look at the rotational structure, not illustrated here, shows that the density of lines is much larger in the OH than in the CH fundamental bands. This is likely to indi-

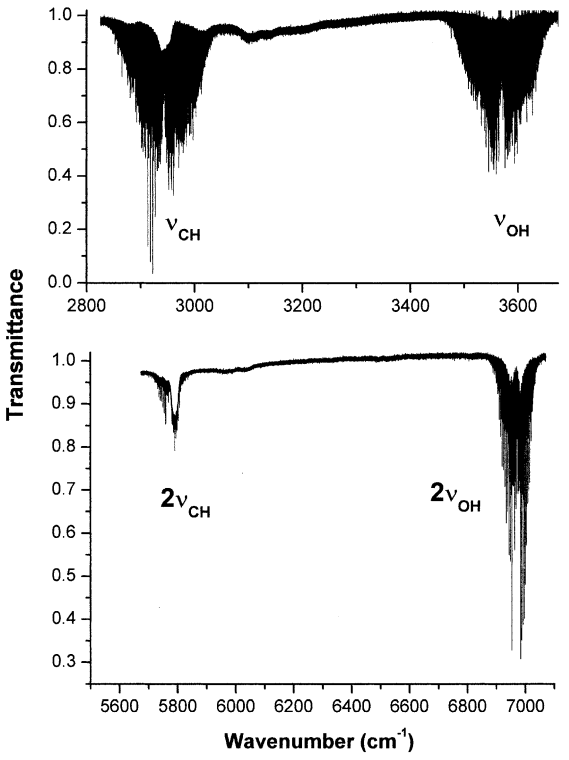

Fig. 7. Transmittance spectrum of *trans*-formic acid in the ground electronic state showing the ranges of the OH and CH stretch fundamentals (upper panel) (240 cm absorption pathlength, 1 hPa pressure), and of their first overtone (lower panel) (240 cm absorption pathlength, 12.3 hPa pressure).

cate the existence of couplings affecting the former band, probably involving the $2\nu_3$, $\nu_2+\nu_7$ and $\nu_2+\nu_9$ close levels. As a result of these resonances, the expected intensity of the OH fundamental band is probably spread over several transitions, thus decreasing the maximum absorption but increasing the line density, as observed. Very recently, the presence of at least three overlapping bands was reported under very cold jet conditions, at 3566.35, 3568.63 and 3570.66 cm^{-1} [48], thus in agreement with the present tentative explanation.

One should eventually note that, although the OH stretching excitation is also localised on a single bond, as for the CH one discussed in the previous section, there is no overlap between monomer and dimer bands in this case. Indeed, the acidic hydrogen is directly participating in the dimer formation and the related OH stretching vibrational frequency is shifted towards lower energy in the dimer, probably around 3000 cm^{-1} [32].

6.2. Rotational analysis

The $3\nu_1$ band at 10202.81 cm^{-1} is a hybrid *a*/*b* type band, as already reported in 1937 [41]. The rotational constants could be precisely predicted from the study of the other OH stretch overtone bands presented in [9]. A total of 458 vibration–rotation lines were assigned, with J/Ka values from 4/3 up to 16/13 in the *a*-type subband and from 5/1 up to 38/14 in the *b*-type subband, and fitted. The resulting upper state constants are listed in Table 4, from a fit performed using a Watsonian in *A*-reduced, I^r representation [30], constraining

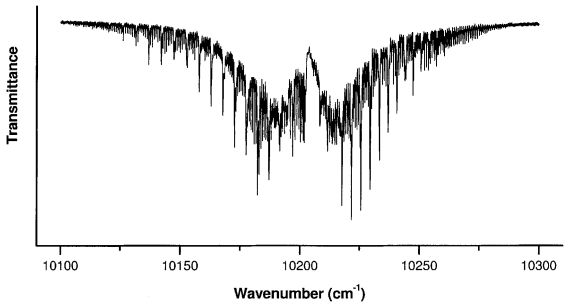

Fig. 8. Portion of the transmittance FT spectrum of *trans*-formic acid in the ground electronic state, showing an overview of the $3\nu_1$ band (4826 cm absorption pathlength, 39 hPa pressure, with 0.03 cm^{-1} FTS resolution). Fringing was artificially removed from the FT spectrum presented (as in Fig. 5).

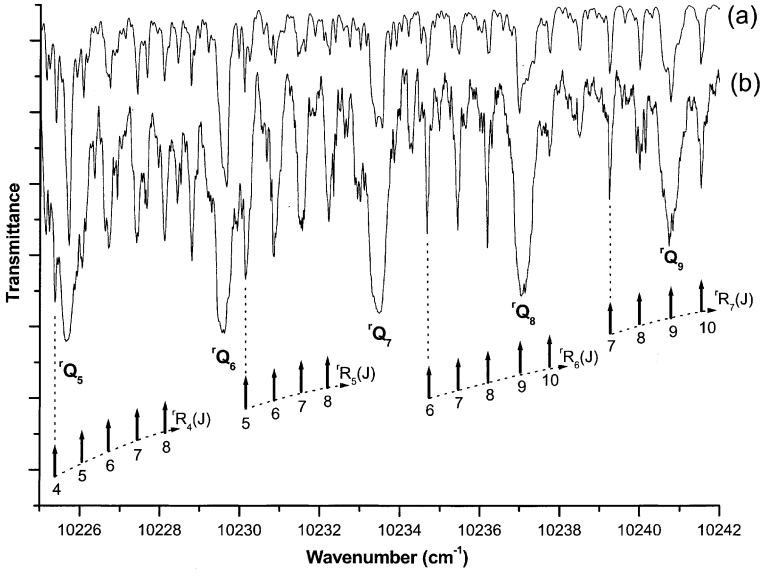

Fig. 9. Detailed line assignments in the *b*-type sub-band of the $3\nu_1$ vibrational band of *trans*-formic acid, with comparison between observed (b) and simulated (a) spectra. The experimental data are from ICLAS (5 km effective absorption pathlength, 1 hPa pressure, with 0.03 cm^{-1} instrumental resolution).

the ground state constants to their values determined in [9]. An overview of the band is provided in Fig. 8. The comparison between observed and simulated spectra is illustrated in Fig. 9, highlighting a range in which local perturbations are less stringent. The most perturbed line positions were not included in the fitting procedure, however still resulting into a standard deviation in the fit as large as about 0.02 cm^{-1}. The line wavenumbers and assignments for the $3\nu_1$ band are available from one of the authors (MH).

7. Conclusions

We have reported on the assignment of all known vibration–rotation bands in the main isotopomer of *trans*-formic acid, in the ground electronic state. Almost all of these bands were observed, between ν_7 at 626 cm^{-1} and $4\nu_1$ at 13284.1 cm^{-1}, in the present work or in a previous of our studies [9], using high-resolution Fourier transform and intracavity laser absorption spectroscopies. Effective vibrational constants were produced and effective rotational analyses were performed for selected bands. The present study has confirmed all trends and problems that can be expected from a high-resolution infrared spectroscopic investigation addressing a small but already sizeable organic compound, in terms of congestion of the rotational structures and of the complexity of the network of resonances. One of the aims of the present study along the line of our recent activities was to test whether we could model these resonances at higher vibrational excitation, using, e.g., the polyad approach, as in acetylene, e.g., [53,54], ethylene [19] or, with limited success, propyne [20]. We were unfortunately unable to achieve this aim, both because of the difficulty of unravelling the vibration–rotation structures and, therefore, because of the lack of reliable and relevant information, and, probably, because of the incommensurability of the vibrational frequencies, ruling out the polyad approach. These problems also illustrate difficulties we encountered with other, larger species, such as, e.g., pyrrole and furan [21]. There is no doubt that jet-cooled instrumental approaches would help producing additional data of interest and will be attempted in a forthcoming study. It is also hoped that such an investigation will generate additional information on the dimer, of which many bands were observed in the present study and only few detailed.

Acknowledgements

We thank Mrs. Rizopoulos (ULB) for help when recording FT spectra and Dr. Perrin (Orsay) for providing information on relative intensities. MF is indebted to ANPCyT (project PICT '98, N° 04155) for financial support. This work was sponsored by EU (contract SPHERS HPRN-CT-2000-00022) and by the Fonds National de la Recherche Scientifique (FNRS-Belgium, contracts FRFC). This research is supported by the Tournesol Integrated Action 02705RM between French Foreign Office and Belgian CGRI and FNRS.

References

[1] K.K. Lehmann, B.H. Pate, G. Scoles, Annu. Rev. Phys. Chem. 45 (1994) 241.
[2] D.J. Nesbitt, R.W. Field, J. Phys. Chem. 100 (1996) 12735.
[3] F.F. Crim, J. Phys. Chem. 100 (1996) 12725.
[4] J.J. Scherer, J.B. Paul, A. O'Keefe, R.J. Saykally, Chem. Rev. 97 (1997) 25.
[5] M. Herman, J. Liévin, J. Vander Auwera, A. Campargue, Adv. Chem. Phys. 108 (1999) 1.
[6] A. Campargue, L. Biennier, A. Garnache, A. Kachanov, D. Romanini, M. Herman, J. Chem. Phys. 111 (1999) 7888.
[7] G. Winnewisser, T. Drascher, T. Giesen, I. Pak, F. Schmülling, R. Schieder, Spectrochim. Acta A55 (1999) 2121.
[8] A. Mellouki, J. Vander Auwera, M. Herman, J. Mol. Spectrosc. 193 (1999) 195.
[9] D. Hurtmans, F. Herregodts, M. Herman, J. Liévin, A.A. Kachanov, A. Campargue, J. Chem. Phys. 113 (2000) 1535.
[10] M. Hepp, R. Georges, M. Herman, J.-M. Flaud, W.J. Lafferty, J. Mol. Struct. 517/518 (2000) 171.
[11] A. Callegari, U. Merker, P. Engels, H.K. Srivastava, K.K. Lehmann, G. Scoles, J. Chem. Phys. 113 (2000) 10583.
[12] J.M. Flaud, W.J. Lafferty, M. Herman, J. Chem. Phys. 114 (2001) 9361.
[13] C. Callegari, K.K. Lehmann, R. Schmied, G. Scoles, J. Chem. Phys. 115 (2001) 100090.
[14] P. Khare, N. Kumar, K.M. Kumari, S.S. Srivastava, Rev. Geophys. 37 (1999) 227.

[15] F.J. Lovas, J. Phys. Chem. Ref. Data 21 (1992) 181.
[16] A.C. Mink, W.M. Irvine, P. Friberg, Astron. Astrophys. 258 (1992) 489.
[17] A. Perrin, C.P. Rinsland, A. Goldman, J. Geophys. Res. D 104 (1999) 18661.
[18] A. Perrin, J.-M. Flaud, J. Vander Auwera, M. Herman, B. Bakri, J. Demaison, J. Mol. Spectrosc., in press.
[19] R. Georges, M. Bach, M. Herman, Mol. Phys. 97 (1999) 279.
[20] M.I. El Idrissi, J. Lievin, M. Herman, A. Campargue, G. Graner, Chem. Phys. 265 (2001) 273.
[21] A. Mellouki, J. Liévin, M. Herman, Chem. Phys. 271 (2001) 239.
[22] M. Herman, R. Georges, M. Hepp, D. Hurtmans, Int. Rev. Phys. Chem. 19 (2000) 277.
[23] I.C. Hisatsune, J. Heicklen, Can. J. Spectrosc. 18 (1973) 135.
[24] W.H. Hocking, Z. Naturforsch. 31a (1976) 1113.
[25] M. Pettersson, J. Lundell, L. Khriachtchev, M. Rasanen, J. Am. Chem. Soc. 119 (1997) 11715.
[26] A. Almenningen, O. Bastiansen, T. Motzfeldt, Acta Chem. Scand. 23 (1969) 2848.
[27] M.D. Harmony, V.W. Laurie, R.L. Kuczkowski, R.H. Schwendeman, D.A. Ramsay, F.J. Lovas, W.J. Lafferty, A.G. Maki, J. Phys. Chem. Ref. Data 8 (1979) 619.
[28] R.W. Davis, A.G. Robiette, M.C.L. Gerry, E. Bjarnov, G. Winnewisser, J. Mol. Spetrosc. 81 (1980) 93.
[29] D. Luckhaus, M. Quack, M. Willeke, Zeit. Phys. Chem. 214 (2000) 1087.
[30] J.K.G. Watson, in: J.R. Durig (Ed.), Vibrational Spectra and Structure. A Series of Advances, Elsevier, Amsterdam, 1977.
[31] H. Morita, S. Nagakura, J. Mol. Spectrosc. 41 (1972) 54.
[32] Y. Marechal, J. Chem. Phys. 87 (1987) 6344.
[33] F. Ito, T. Nakanaga, Chem. Phys. Lett. 318 (2000) 571.
[34] W. Qian, S. Krimm, J. Phys. Chem. A 105 (2001) 5046.
[35] M.J. Frisch et al. Gaussian 98, Revision A.7, Gaussian Inc., Pittsburgh PA, 1998.
[36] M. Takami, K. Shimoda, Jpn. Appl. Phys. 13 (1974) 1699.
[37] W.H. Weber, P.D. Maker, J. Mol. Spectrosc. 121 (1987) 243.
[38] R.E. Bumgarner, J.I. Choe, S.G. Kukolich, R.J. Butcher, J. Mol. Spectrosc. 132 (1988) 261.
[39] T.L. Tan, K.L. Goh, P.P. Ong, H.H. Teo, J. Mol. Spectrosc. 202 (2000) 194.
[40] G. Weirauch, A.A. Kachanov, A. Campargue, M. Bach, M. Herman, J. Vander Auwera, J. Mol. Spectrosc. 202 (2000) 98.
[41] S.H. Bauer, R.M. Badger, J. Chem. Phys. 5 (1937) 852.
[42] J.K. Wilmhurst, J. Chem. Phys. 25 (1956) 478.
[43] R.C. Millikan, K.S. Pitzer, J. Chem. Phys. 27 (1957) 1305.
[44] T. Miyazawa, K.S. Pitzer, J. Chem. Phys. 30 (1959) 1076.
[45] K. Nakamoto, S. Kishida, J. Chem. Phys. 41 (1964) 1554.
[46] R.L. Redington, J. Mol. Spectrosc. 65 (1977) 171.
[47] G.M.R.S. Luiz, A. Scalabrin, D. Pereira, Inf. Phys. Tech. 38 (1997) 45.
[48] F. Madeja, M. Havenith-Newen, K. Nauta, R.E. Miller, in: 17th Colloquium on High Resolution Molecular Spectroscopy, Nijmegen, 9–13 September, poster D6, 2001, p. 96.
[49] H. Kuze, T. Amano, T. Shimizu, J. Chem. Phys. 77 (1982) 714.
[50] T. Baba, T. Tanaka, I. Morino, K.M.T. Yamada, K. Tanaka, J. Chem. Phys. 110 (1999) 431.
[51] O. Boyarkin, T. Rizzo, D. Perry, J. Chem. Phys. 110 (1999) 11359.
[52] M. Herman, F. Herregodts, R. Georges, M. Hepp, I. Hadj Bachir, M. Lecoutre, I. Kleiner, Chem. Phys. 246 (1999) 433.
[53] M.I. El Idrissi, J. Liévin, A. Campargue, M. Herman, J. Chem. Phys. 110 (1999) 2074.
[54] B.I. Zhilinskii, M.I. El Idrissi, M. Herman, J. Chem. Phys. 113 (2000) 7885.